ACS APPLIED MATERIALS & INTERFACES

Research Article

www.acsami.org

# Polarity Engineering of Conjugated Polymers by Variation of Chemical Linkages Connecting Conjugated Backbones

Hui-Jun Yun,[†] Hyun Ho Choi,[‡] Soon-Ki Kwon,*[,†] Yun-Hi Kim,*[,§] and Kilwon Cho*[,‡]

[‡]Department of Chemical Engineering and Center for Advanced Soft Electronics, Pohang University of Science and Technology (POSTECH), Pohang 790-784, Korea

[†]School of Materials Science and Engineering and Research Institute for Green Energy Convergence Technology (REGET), Gyeongsang National University, Jinju 660-701, Korea

[§]Department of Chemistry, Gyeongsang National University and Research Institute of Nature Science (RINS), Jinju 660-701, Korea

Supporting Information

**ABSTRACT:** The fine tuning of the dominant polarity in polymer semiconductors is a key issue for high-performance organic complementary circuits. In this paper, we demonstrate a new methodology for addressing this issue in terms of molecular design. In an alternating conjugated donor−acceptor copolymer system, we systematically engineered the chemical linkages that connect the aromatic units in donor moieties. Three donor moieties, thiophene−vinylene−thiophene (TVT), thiophene−acetylene−thiophene (TAT), and thiophene−cyanovinylene−thiophene (TCNT), were combined with an acceptor moiety, thienoisoindigo (TIID), and finally, three novel TIID-based copolymers were synthesized: PTIID−TVT, PTIID−TAT, and PTIID−TCNT. We found that the vinylene, acetylene, and cyanovinylene linkages decisively affect the energy structure, molecular orbital delocalization, microstructure, and, *most importantly*, the dominant polarity of the polymers. The vinylene-linked PTIID−TVT field-effect transistors (FETs) exhibited intrinsic hole and electron mobilities of 0.12 and $1.5 \times 10^{-3}$ $cm^2$ $V^{-1}$ $s^{-1}$, respectively. By contrast, the acetylene-linked PTIID−TAT FETs exhibited significantly improved intrinsic hole and electron mobilities of 0.38 and 0.03 $cm^2$ $V^{-1}$ $s^{-1}$, respectively. Interestingly, cyanovinylene-linked PTIID−TCNT FETs exhibited reverse polarity, with hole and electron mobilities of 0.07 and 0.19 $cm^2$ $V^{-1}$ $s^{-1}$. As a result, the polarity balance, which is quantified as the electron/hole mobility ratio, was dramatically tuned from 0.01 to 2.7. Our finding demonstrates a new methodology for the molecular design of high-performance organic complementary circuits.

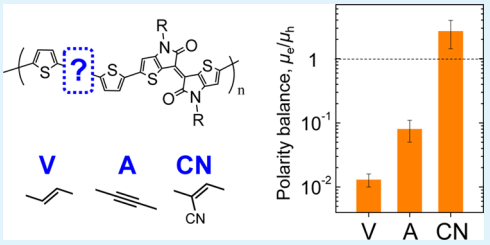


**KEYWORDS:** *thienoisoindigo, chemical linkage, polarity, organic transistor, ambipolarity*

## INTRODUCTION

Organic field-effect transistors (OFETs) have received significant attention because of their high potential in low-cost, large-area, and flexible electronic devices via solution processes.[1−4] A number of studies have sought to improve device performance.[5−9] Among these efforts, recently introduced low-band-gap copolymers based on alternating conjugated donor−acceptor (D−A) dyads have been found to remarkably improve field-effect mobilities.[10−12] The intramolecular charge transfer within such D−A systems, namely, the push−pull effect, can be readily manipulated with endless permutations to yield high-charge-carrier mobilities.[13,14]

These D−A copolymers are typically categorized according to their acceptor building blocks. Acceptor moieties such as diketopyrrolopyrrole (DPP),[15−17] naphthalene diimide (NDI),[18−20] isoindigo (IID),[21,22] and thienoisoindigo (TIID)[23−25] have received significant attention owing to the superior electrical performance of copolymers derived from them. With a fixed acceptor conjugated moiety, many molecular structures have been reported to improve the intra- or interchain charge transport of the resultant polymers. The novelty of these structures is typically attributed to the addition, branching, length control, or new chemical moieties in the side chain or to the number control or new architecture of cyclic aromatic units in the donor part.[26−30] Recently, the groups of Liu and Kim reported new DPP-based polymers whose novelty was not attributed to the aforementioned categories.[31−33] They replaced the single bond that connects thiophenes in the donor part with a vinylene linkage. This strategy improved the rigidity of the conjugated backbone, enabling extended $\pi$ conjugation and a record carrier mobility. This type of an approach, i.e., engineering chemical linkages by connecting donor units, has a sufficient potential for controlling the electrical properties of synthesized polymer-based devices. First, since the modified chemical linkages are located in the conjugated backbone, their electron-donating or electron-withdrawing nature can noticeably affect the band structures and intrinsic intrachain charge transport. Second, these linkages determine the rigidity of the

Received: January 5, 2015
Accepted: February 26, 2015
Published: February 26, 2015





DOI: 10.1021/acsami.5b00073
ACS Appl. Mater. Interfaces 2015, 7, 5898−5906

entire polymer chain, which results in a change in the solubility and solid-state microstructure of the synthesized polymers.

In this paper, we first systematically engineered the chemical linkages in the donor moieties and then synthesized novel TIID-based polymers for investigating the relationship between the chemical linkages and the properties of conjugated organic semiconductors. The chemical linkages were vinylene, acetylene, and cyanovinylene, resulting in thiophene−vinylene−thiophene (TVT), thiophene−acetylene−thiophene (TAT), and thiophene−cyanovinylene−thiophene (TCNT) donor moieties, respectively (Figure 1a). The sp-hybridized

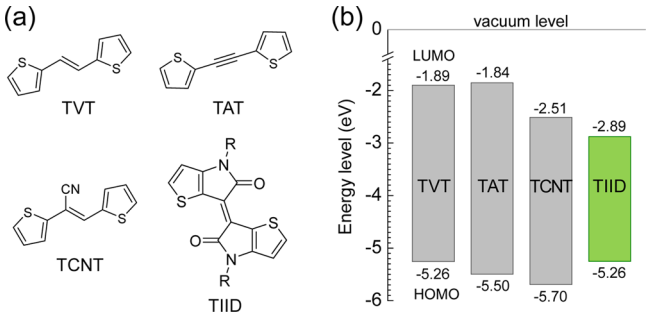


**Figure 1.** (a) Molecular structure of the donor moieties of vinylene-linked TVT, acetylene-linked TAT, and cyanovinylene-linked TCNT and the acceptor moiety of TIID. (b) DFT-calculated energy level diagrams of the donor and acceptor moieties.

carbons in the acetylene linkage have more electron-withdrawing nature than the $sp^2$-hybridized carbons in the vinylene linkage.[34,35] Although cyanovinylene and vinylene have similar backbone structures, the cyano group can strongly attract electrons to the neighboring vinylene linkage. The LUMO and HOMO levels of the donor moieties were also consistent with our expectation. Density functional theory (DFT) calculations showed that the LUMO and HOMO levels of TAT and TCNT were deeper than those of TVT (Figure 1b). The energy structures of the synthesized polymers PTIID−TVT, PTIID−TAT, and PTIID−TCNT followed the same tendency as those of the donor moieties. Most importantly, the polarity balance was dramatically tuned in FET devices; the electron/hole mobility ratio varied from 0.01 to 2.7. In particular, PTIID−TCNT FETs exhibited *n*-channel dominant characteristics. Our findings demonstrate a new methodology for the molecular design of high-performance organic complementary circuits.

## SYNTHESIS AND CHARACTERIZATION

The syntheses of the monomers and polymers are shown in Scheme 1. TIID with C29 alkyl groups and a C6 linear space was synthesized by N-arylation, acylation, dimerization, and bromination. Polymerization was conducted by Stille coupling with distannylated TVT, TAT, and TCNT. After sequential Soxhlet purification with methanol, acetone, hexane, toluene, and chloroform, the polymers were obtained from precipitation in methanol. These polymers were found to be highly soluble in common organic solvents such as chloroform, chlorobenzene, and dichlorobenzene. The weight-average molecular weights ($M_w$) of PTIID−TVT, PTIID−TAT, and PTIID−TCNT were 42.3, 55.1, and 87.1 kDa, respectively; their corresponding polydispersities were 1.84, 1.67, and 1.87. The thermal properties of the polymers were examined by differential scanning calorimetry (DSC) and thermogravimetric analysis (TGA). The polymers did not display any transition up to 250 °C in their DSC curves (see Supporting Information), while they exhibited good thermal stability with 5% decomposition at temperatures higher than 367 °C in their TGA curves (see Supporting Information).

**Scheme 1. Synthetic Procedures of PTIID−TVT, PTIID−TAT, and PTIID−TCNT**

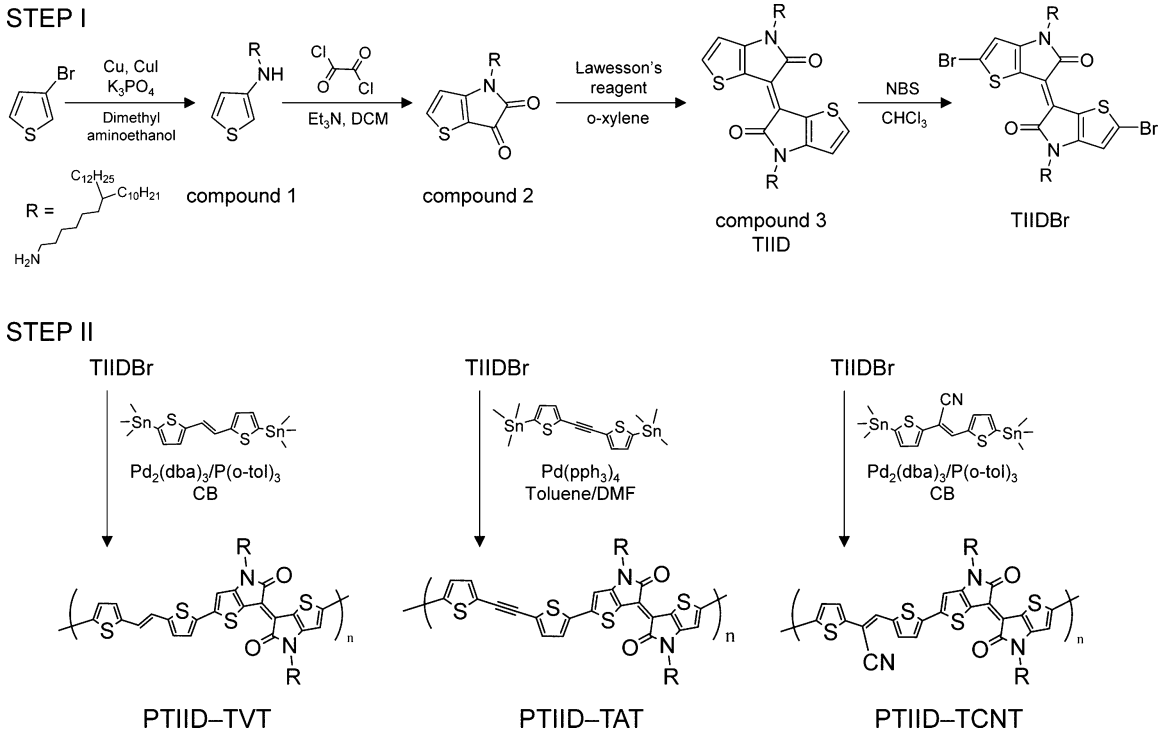




DOI: 10.1021/acsami.5b00073
ACS Appl. Mater. Interfaces 2015, 7, 5898−5906

## ELECTROCHEMICAL AND OPTICAL PROPERTIES

Cyclic voltammetry (CV) measurements were conducted to investigate the band structure of each polymer (Figure 2a). The

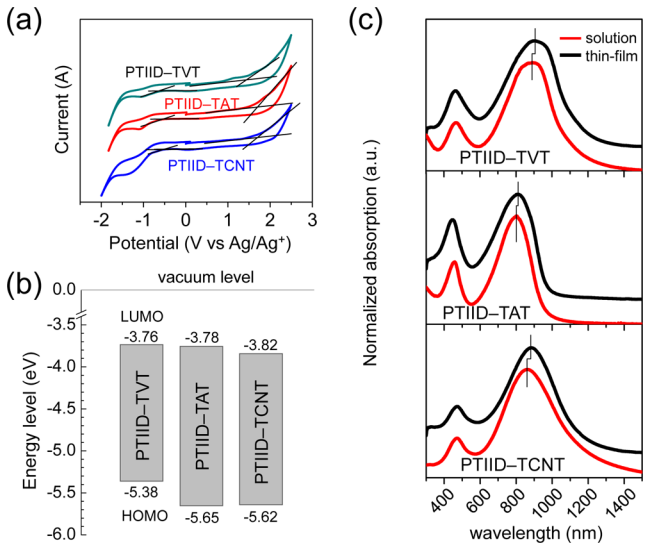


**Figure 2.** (a) Cyclic voltammograms, (b) electrochemical energy diagrams, and (c) UV–vis absorption spectra of the polymers.

energy levels were estimated using a previously reported empirical equation. The LUMO and HOMO levels of the synthesized polymers are summarized in Figure 2b and Table 1.

**Table 1. Band Structures, i.e., LUMO, HOMO, and Band Gap, Obtained from Cyclic Voltammograms and UV–Vis Absorption Peaks of the Synthesized Polymers**

| polymer | LUMO (eV) | HOMO (eV) | band gap (eV) | $\lambda_{max}^{soln}$ (nm) | $\lambda_{max}^{film}$ (nm) |
|---|---|---|---|---|---|
| PTIID-TVT | −3.76 | −5.38 | 1.62 | 890 | 903 |
| PTIID-TAT | −3.78 | −5.65 | 1.87 | 802 | 809 |
| PTIID-TCNT | −3.82 | −5.62 | 1.80 | 861 | 882 |

The energy levels for the synthesized polymers had a similar tendency to those for the donor moieties. The HOMO and LUMO levels were significantly deeper in PTIID–TAT and PTIID–TCNT than in PTIID–TVT, possibly due to the relatively strong electron-accepting nature of the acetylene- and cyanovinylene-linked donor moieties. In particular, PTIID–TCNT exhibited the lowest LUMO level near −4.0 eV, indicating the potential of facile electron injection from electrodes and *n*-channel formation in FET devices.

The UV–vis absorption spectra of the polymers also followed the same tendency as the CV curves (Figure 2c). The polymers commonly exhibited dual-band absorption; their absorption maxima ($\lambda_{max}$) are summarized in Table 1. From solution to film, all materials exhibited a red shift of absorption maxima, which has been typically observed in polymer semiconductors. However, it is quite weak ($\Delta\lambda_{max}$ = 7–21 nm). It is presumably because the conjugated backbone was sufficiently rigid by the vinylene or acetylene linkages, so it preserves the coplanar form even in the solution phase.[36−38] The strong blue shifts from PTIID–TVT to PTIID–TAT and PTIID–TCNT were attributed to the aforementioned deepened HOMO levels. The optical band gaps were narrower (0.4–0.6 eV) than the electrochemically determined gaps, possibly due to the exciton binding energy of the conjugated polymers (estimated to range between 0.4 and 1.0 eV).[39,40]

## THEORETICAL CALCULATIONS

To gain insight into the structural and electronic features of PTIID-based polymers, molecular orbital distributions under various chain conformations were estimated by a DFT calculation method at the B3LYP/6-31G level.[41] For further estimation, it is vital to compare the molecular orbitals around the engineered chemical linkages;[42] hence, we constructed model molecules having TIID–donor–TIID as the skeletal structure. Since the alkyl side chains do not significantly contribute to the variations in molecular orbitals, they were removed from the model molecules. First, the optimized structure according to energy minimization was obtained, as shown in Figure 3a. Coplanarity was favored in all polymers; dihedral angles between the donor moieties and TIID were below 0.1°. These coplanar forms are estimated to facilitate intermolecular $\pi$–$\pi$ interaction and crystalline domain formation. The LUMO and HOMO levels were essentially consistent with the aforementioned trends, which are based on the optical and electrochemical properties of the polymers. Furthermore, both LUMO and HOMO orbitals were well delocalized over the entire conjugated backbone.

In addition, we calculated the molecular orbital distributions of the model molecules under chain twist; this is essential because the conjugated polymer thin films produced by a typical spin-coating process inevitably have amorphous phases and tie molecules with many degrees of conformational freedom, resulting in complex microstructures in the solid state. These regions play a vital role in determining the charge transport in the entire film.[43−45] Even though the coplanar state is energetically favored in all synthesized polymers, tie molecules cannot maintain a coplanar state for connecting crystalline domains and thermal energy is sufficient to induce small twists of monomer units.[35] The molecular structures and orbitals of the twisted chains are shown in Figure 3b. Because the engineered chemical linkages are key positions in this study, T–V, T–A, and T–CN bonds were twisted. The HOMO orbitals of all polymers maintained delocalization along the conjugated backbones under chain twist. Interestingly, the LUMO distribution of PTIID–TVT was sensitive to chain twist, whereas those of PTIID–TAT and PTIID–TCNT were highly insensitive. The well-distributed LUMO isosurface of PTIID–TVT in the coplanar state became localized under chain twist; the charge density of the left side from the T–V bond was visibly decreased. In contrast, the LUMO isosurfaces of PTIID–TAT and PTIID–TCNT in the coplanar state maintained their delocalization even under chain twist. This result indicates that intrachain electron transport is prone to interruption by twisting of the T–V bond; however, it is highly insensitive to twisting of the T–A and T–CN bonds. Therefore, ambipolar charge transport was expected in PTIID–TAT and PTIID–TCNT FETs, and unipolar or low electron mobility was expected in PTIID–TVT FETs.

Actually, high twist angles such as 45–90° are not energetically possible (Figure S13, Supporting Information). Under the low twist angles of the T–V, T–A, or T–CN bonds, the HOMO and LUMO isosurfaces can maintain their delocalization in a monomer unit but the delocalization of the LUMO must be more weakened than that of the HOMO. This difference will be noticeably increased as the number of


DOI: 10.1021/acsami.5b00073
ACS Appl. Mater. Interfaces 2015, 7, 5898–5906

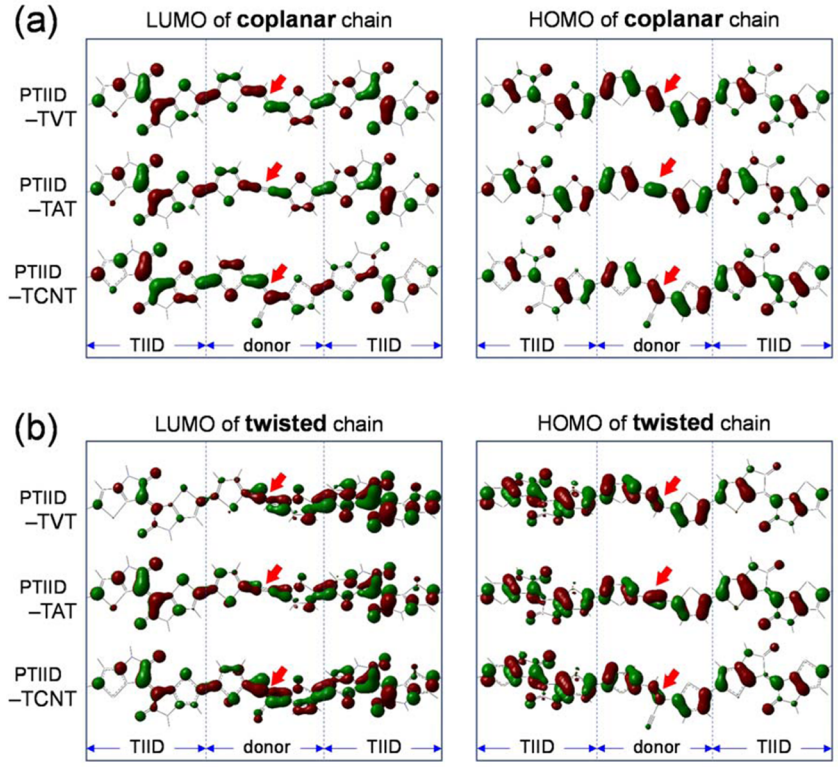


**Figure 3.** DFT-calculated molecular orbital distributions of the model structures corresponding to PTIID−TVT, PTIID−TAT, and PTIID−TCNT under the various degrees of chain conformation (B3LYP/6-31G, isovalue = 0.028). (a) DFT-optimized coplanar chains. (b) Twisted chains from the optimized state in which the thiophene−vinylene bond for PTIID−TVT, thiophene−acetylene bond for PTIID−TAT, and thiophene−cyanovinylene bond for PTIID−TCNT were twisted to 45°. Vinylene, acetylene, and cyanovinylene linkages are located at the center of model structures, as highlighted by red arrows.

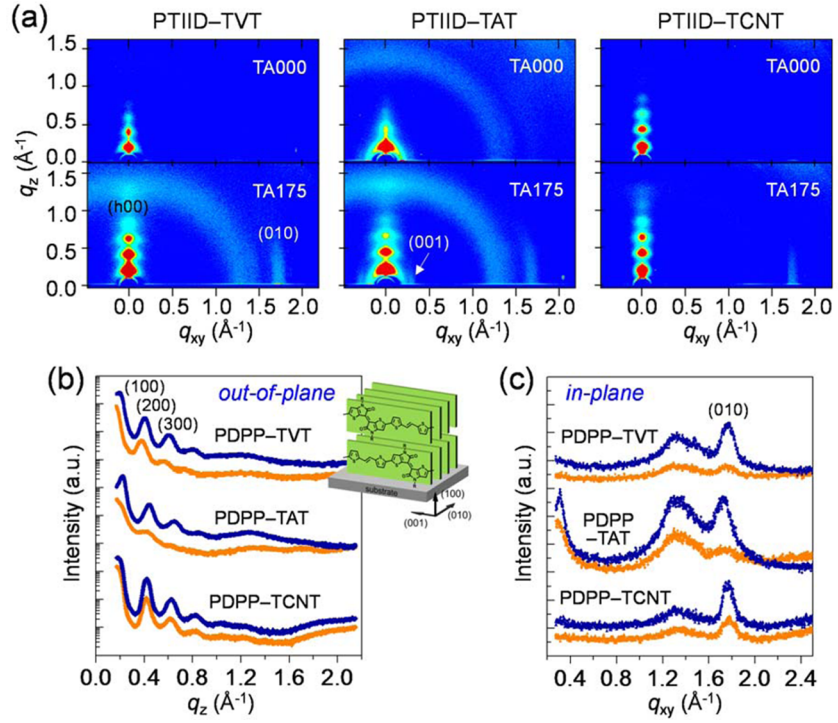


**Figure 4.** Crystalline nature and molecular orientation of the synthesized polymer films before and after thermal annealing at 175 °C (before TA000; after TA175). (a) Two-dimensional grazing incidence X-ray diffraction (2D-GIXD) patterns. (b) The definition of crystalline planes and edge-on structure relative to the substrate. (b) Out-of-plane ($q_{xy}$ = 0) and (c) in-plane ($q_z$ = 0) X-ray diffraction patterns (orange, TA000; blue, TA175). (Inset scheme in b) Definition of crystalline planes and edge-on structure relative to the substrate.



DOI: 10.1021/acsami.5b00073
*ACS Appl. Mater. Interfaces* 2015, 7, 5898−5906

the twisted monomer unit increases. Because a large twist of a polymeric chain in tie−molecular regions can arise as the sum of the small twists of the monomer units, the LUMO isosurfaces in tie−molecular regions lose their delocalization, whereas the HOMO isosurfaces can still maintain their delocalization. It can result in unfavorable electron transport between the crystalline domains and low electron mobility for PTIID−TVT FETs.

## MICROSTRUCTURE ANALYSIS

We performed two-dimensional grazing incident X-ray diffraction (2D-GIXD) analysis to investigate the crystalline nature and molecular orientation of the synthesized polymers.[46−48] As-spun and annealed thin films spin coated on Cytop-modified $SiO_2$/Si substrates were prepared. 2D-GIXD patterns and the corresponding one-dimensional profiles are shown in Figure 4, and the extracted crystallographic parameters are summarized in Table 2. All PTIID-based polymer thin films exhibited edge-on orientation of the substrate regardless of post-treatment; ($h$00) and (010) diffraction peaks were predominantly observed along the out-of-plane ($q_z$) and in-plane ($q_{xy}$) directions, respectively. By thermal annealing, these peaks were noticeably intensified, implying the increased crystallinity in the films. Furthermore, the $q$ values of them became higher, indicating the close intermolecular stacking.

**Table 2. Crystallographic Parameters of the Synthesized Polymers[a]**

| | | $d$ spacing [Å] | | |
|---|---|---|---|---|
| polymer | annealing temp [°C] | (100) | (010) | (001) |
| PTIID−TVT | N/A | 33.30 | 3.59 | |
| | 175 | 31.02 | 3.54 | |
| PTIID−TAT | N/A | 29.80 | 3.62 | |
| | 175 | 28.72 | 3.62 | 20.33 |
| PTIID−TCNT | N/A | 30.36 | 3.55 | |
| | 175 | 30.22 | 3.55 | |

[a](100) peaks were assigned from out-of-plane diffraction patterns, and the other peaks were assigned from in-plane diffraction patterns.

Concerning the (010) peaks related to $\pi-\pi$ stacking distance, PTIID−TVT and PTIID−TCNT exhibited closer $\pi-\pi$ stacking as compared with PTIID−TAT. The vinylene linkage exhibited a closer intermolecular $\pi-\pi$ stacking as compared with the acetylene linkage in the polymer backbone, which is consistently observed in DPP-based polymers.[35,49] This subtle but reproducible interplay in the molecular packing was attributed to the difference of backbone geometries. The acetylene linkages might have contributed to the formation of relatively linear TAT units, which were found to be energetically more favorable to the chain twist than in TVT and TCNT units.[35] This relatively favorable chain twist plays an unfavorable role in the intermolecular $\pi-\pi$ stacking, resulting in more distant (010) stacking of PTIID−TAT compared with that of PTIID−TVT and PTIID−TCNT. On the other hand, PTIID−TAT thin films exhibited an additional strong diffraction peak at $q_{xy}$ = 0.31 Å$^{-1}$ along the in-plane direction that was not observed for the other polymer thin films. This peak corresponds to a $d$ spacing of 20.33 Å, which matches well to the end-to-end distance of the coplanar PTIID−TAT monomer backbone (20.78 Å). This strong (001) peak implies that the PTIID−TAT thin film contains well-stretched polymeric chains separated by a longer distance in comparison with PTIID−TVT and PTIID−TCNT thin films. This result indicates that the acetylene linkage exerts a positive effect on intramolecular charge transport. Interestingly, the PTIID−TCNT and PTIID−TVT thin films exhibited similar diffraction patterns and intermolecular packing distances even though the backbone structure of cyanovinylene is rather asymmetric as compared with that of vinylene. It indicates that the lack of symmetry by the incorporation of the cyanovinylene linkages negligibly affects intermolecular packing.

## ORGANIC TRANSISTOR PERFORMANCE

To investigate the relationship between the structures and the electrical properties, top-contact bottom-gate FETs were fabricated. Cytop-treated $SiO_2$ with a capacitance of 8.1 nF cm$^{-2}$ was used as a gate dielectric, and 50 nm thick patterned Au layers were used as source and drain electrodes. It is well known that Cytop thin films form defect-free surfaces; hence, Cytop-based FETs are expected to exhibit near-intrinsic electrical properties of the synthesized polymers.[50−53] Warm solutions of the synthesized polymers in chloroform (5 mg mL$^{-1}$ at 55 °C) were dropped onto the substrate and then spin coated in a nitrogen-purged glovebox. The details of device fabrication are provided in the experimental section. The typical transfer curves of PTIID-based polymer FETs are shown in Figure 5a, and their quantitative electrical properties are summarized in Table 3. Both $p$-mode ($V_G$, $V_D$ < 0) and $n$-mode ($V_G$, $V_D$ > 0) sweeps were performed in the saturation regime to examine the dominant polarity of the devices. All PTIID-based polymer FETs exhibited the enhancement of carrier mobilities by thermal annealing, which was attributed to the increased crystallinity and the closer intermolecular stacking observed in the 2D-GIXD analysis. Furthermore, they exhibited ambipolar charge transport. However, PTIID−TAT and PTIID−TCNT FETs produced more V-shaped transfer curves than PTIID−TVT FETs, and in particular, PTIID−TCNT FETs produced almost symmetric V-shaped transfer curves. The polarity balance between electron and hole mobilities ($\mu_e$ and $\mu_h$), which is quantified as the $\mu_e/\mu_h$ ratio, varied remarkably: 0.01 for PTIID−TVT FETs, 0.08 for PTIID−TAT FETs, and 2.7 for PTIID−TCNT FETs (Figure 5d). As shown in Figure 5b, the output curves of the PTIID−TAT and PTIID−TCNT FETs indicate relatively ambipolar charge transport in contrast to that of PTIID−TVT FETs. This remarkable change in the polarity balance predominantly originated from the variation of electron mobilities, as shown in Figure 5c. PTIID−TVT exhibited the lowest electron mobility of 1.5 × 10$^{-3}$ cm$^2$ V$^{-1}$ s$^{-1}$ among the synthesized polymers, and PTIID−TAT exhibited 20 times higher electron mobility of 0.03 cm$^2$ V$^{-1}$ s$^{-1}$. PTIID−TCNT exhibited the highest electron mobility of 0.19 cm$^2$ V$^{-1}$ s$^{-1}$. The higher polarity balances and remarkably higher electrical mobilities of PTIID−TAT and PTIID−TCNT compared to PTIID−TVT presumably resulted from the former polymers having well-delocalized LUMO orbitals, which are insensitive to the chain twist around the acetylene and cyanovinylene linkages as predicted by DFT calculations. This result implies that PTIID−TAT and PTIID−TCNT, as compared with PTIID−TVT, allow more facile electron transport along their twisted intrachains, which are formed in the amorphous and tie−molecular regions. The turn-on voltages lying on the border between the hole and the electron accumulations in the transfer curves followed a consistent trend with the carrier mobilities.


DOI: 10.1021/acsami.5b00073
ACS Appl. Mater. Interfaces 2015, 7, 5898−5906

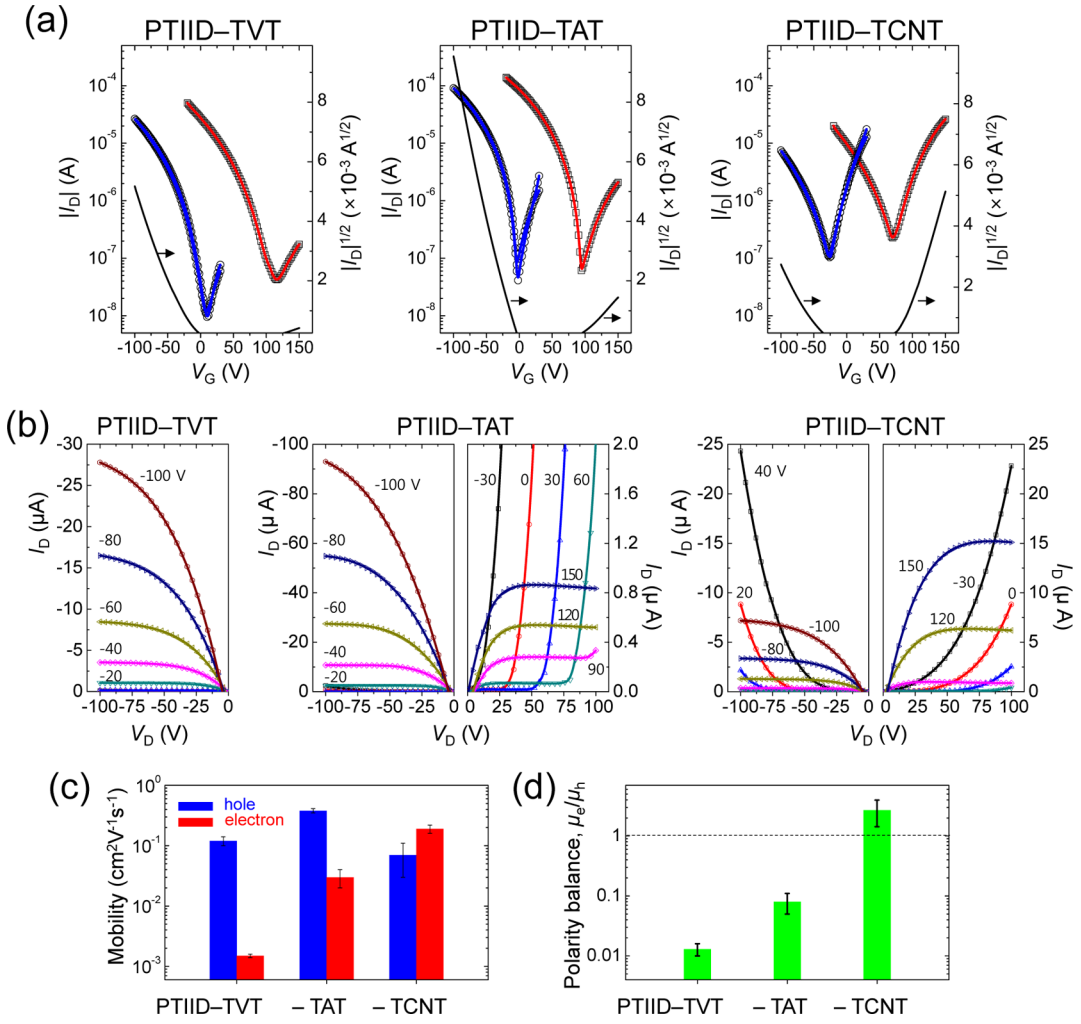


**Figure 5.** Electrical properties of the synthesized polymer-based FETs with thermal annealing post-treatment. (a) Transfer characteristic curves: *p*-channel accumulation mode (blue circle) with $V_D$ = −100 V, and *n*-channel accumulation mode (red square) with $V_D$ = 100 V. (b) Output characteristic curves. (c) Average hole and electron mobilities. (d) Polarity balance, quantified as electron/hole mobility ratio ($\mu_e/\mu_h$).

**Table 3. Summary of Field-Effect Mobilities and Activation Energies of the Synthesized Polymer FETs**

| | | *p* channel | | *n* channel | | |
|---|---|---|---|---|---|---|
| polymer | annealing temp. [°C] | $\mu_{h,ave}$ [$cm^2$ $V^{-1}$ $s^{-1}$] | $E_A$ [meV] | $\mu_{e,ave}$ [$cm^2$ $V^{-1}$ $s^{-1}$] | $E_A$ [meV] | $\mu_e/\mu_h$ |
| PTIID−TVT | N/A | 0.06 (±0.02) | | $1.1(\pm0.3) \times 10^{-4}$ | | $1.8 \times 10^{-2}$ |
| | 175 | 0.12 (±0.02) | 10.35 | $1.5(\pm0.1) \times 10^{-3}$ | | $1.3 \times 10^{-2}$ |
| PTIID−TAT | N/A | 0.10 (±0.02) | | $5.8(\pm0.3) \times 10^{-3}$ | | 0.06 |
| | 175 | 0.38 (±0.03) | 8.24 | 0.03 (±0.01) | 11.02 | 0.08 |
| PTIID−TCNT | N/A | 0.03 (±0.01) | | 0.07 (±0.02) | | 2.4 |
| | 175 | 0.07 (±0.04) | 12.16 | 0.19 (±0.03) | 10.32 | 2.7 |

PTIID−TCNT FETs exhibited negatively shifted turn-on voltages as compared with PTIID−TVT and PTIID−TAT, indicating the favorable formation of electron-accumulated channels. Interestingly, in contrast with PTIID−TVT and PTIID−TAT, PTIID−TCNT exhibited reverse polarity, presumably as a result of the strong electron-withdrawing nature of the cyanovinylene linkage inserted in the donor part. Furthermore, it is indicative of the importance of chemical linkages for polarity tuning. The $\mu_e/\mu_h$ ratio of 2.7 for PTIID−TCNT is comparable to actual Si-based CMOS devices with a $\mu_e/\mu_h$ ratio of ∼2.

The PTIID−TAT FETs exhibited the highest hole mobility, with average and maximum values of 0.38 and 0.43 $cm^2$ $V^{-1}$ $s^{-1}$, respectively. This performance was attributed to the unique (001) diffraction peak of the PTIID−TAT thin film, which was not observed in PTIID−TVT and PTIID−TCNT thin films. The strong (001) diffraction peak is indicative of the well-stretched polymer backbone, consequently permitting facile intrachain charge transport.

Transfer measurements were conducted under various temperatures to understand the charge transport mechanism of PTIID-based polymer FETs. The temperature was varied from 305 to 115 K in UHV (∼$10^{-6}$ Torr). The measured mobility−temperature relationship is shown in Figure 6 and Table 3. Both hole and electron mobilities of all devices were saturated at high temperature and continuously decreased with


DOI: 10.1021/acsami.5b00073
ACS Appl. Mater. Interfaces 2015, 7, 5898−5906

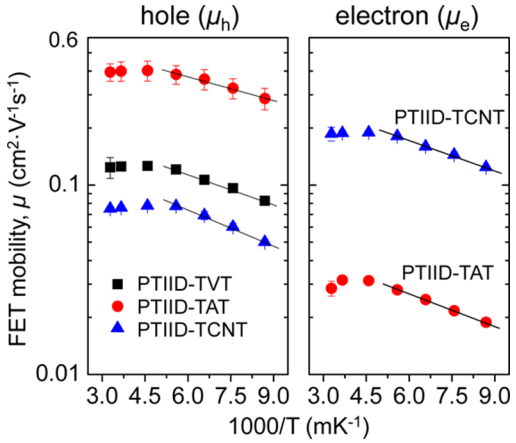


**Figure 6.** Temperature dependence of field-effect mobilities (FET mobilities) of PTIID−TVT-, PTIID−TAT-, and PTIID−TCNT-based FETs. Temperature range is 115−305 K. Activation energy, $E_A$, was obtained by using multiple trapping and release model, $\mu(T) = \mu_0 \exp(-E_A/kT)$.

temperature at low temperature. As shown in Figure 6, the carrier mobilities exhibited an Arrhenius dependency at low temperature, consistent with the charge transport mechanism of the multiple-trapping-and-release model; $\mu(T) = \mu_0 \exp(-E_A/kT)$, where $E_A$ is the activation energy for releasing the trapped charge.[54,55] Quite shallow traps in the range of 8.2−12.2 meV were formed in the devices. In this range, the carriers can easily overcome these traps at high temperature by utilizing their thermal energy; hence, intrinsic band-like transport representing the saturated mobilities was observed at high temperature. We argue that the intrinsic charge transport properties of the synthesized polymer thin films were observed in our devices.[55−57] Furthermore, the tendency of the activation energies was observed to consistently follow that of carrier mobilities; PTIID−TAT exhibited the lowest activation energy for holes (8.2 meV), and PTIID−TCNT exhibited the highest activation energy for holes (12.2 meV) but the lowest activation energy for electrons (10.3 meV). This presumably indicates that the depth of shallow traps in these devices affects carrier transport even in the band-like transport regime by subtly affecting the scattering time of mobile carriers.

## CONCLUSION

Fine polarity tuning of organic semiconductors is a key issue for organic complementary circuits. Here we demonstrated that modification of the chemical linkages in the conjugated backbone of polymer semiconductors was a noteworthy approach. The synthesized polymers PTIID−TVT, PTIID−TAT, and PTIID−TCNT exhibited energy structures that were dependent on the electron-withdrawing strength of the chemical linkages. The acetylene linkages in PTIID−TAT straightened the conjugated backbones, which contributed to facile intrachain charge transport and the highest hole mobility among the synthesized polymers. More importantly, the acetylene and cyanovinylene linkages enabled twist-insensitive charge transport, thereby making electron transport between crystalline domains significantly more favorable in PTIID−TAT and PTIID−TCNT FETs. As a result, the polarity balance, which is quantified as the $\mu_e/\mu_h$ ratio, remarkably varied from 0.01 for PTIID−TVT FETs, to 0.08 for PTIID−TAT FETs, and to 2.7 for PTIID−TCNT FETs. Our approach can also be applied to DPP-, IID-, NDI-, and new acceptor-based polymer systems for high-performance organic electronic devices, particularly for tuning the dominant polarity.

## ASSOCIATED CONTENT

### Supporting Information

Detailed synthetic procedures, characterization of all intermediate compounds, and AFM morphologies of thin films. This material is available free of charge via the Internet at http://pubs.acs.org.

## AUTHOR INFORMATION

### Corresponding Authors

*E-mail: skwon@gnu.ac.kr.
*E-mail: ykim@gnu.ac.kr.
*E-mail: kwcho@postech.ac.kr.

### Author Contributions

H. H. Choi and H.-J. Yun contributed equally; S.-K. Kwon, Y.-H. Kim, and K. Cho designed the molecular structure and supervised this work; H.-J. Yun wrote the paper, synthesized the polymers, and performed the basic characterizations; H. H. Choi wrote the paper and performed DFT calculation, device fabrication, and analysis of microstructures and FET performances.

### Notes

The authors declare no competing financial interest.

## ACKNOWLEDGMENTS

This work was supported by a grant (Code Nos. 2011-0031628 and 2012M3A6A5055225) from the Center for Advanced Soft Electronics under the Global Frontier Research Program of the Ministry of Science, ICT & Future Planning, Korea. The 2D-GIXD data were obtained at 3C and 9A beamlines, Pohang Accelerator Laboratory.

## REFERENCES

(1) Klauk, H. Organic Thin-Film Transistors. *Chem. Soc. Rev.* **2010**, *39*, 2643−2666.
(2) Kang, B.; Lee, W. H.; Cho, K. Recent Advances in Organic Transistor Printing Processes. *ACS Appl. Mater. Interfaces* **2013**, *5*, 2302−2315.
(3) Horowitz, G. The Organic Transistor: State-of-the-Art and Outlook. *Eur. Phys. J. Appl. Phys.* **2011**, *53*, 33602.
(4) Muccini, M. A Bright Future for Organic Field-Effect Transistors. *Nat. Mater.* **2006**, *5*, 605−613.
(5) Briseno, A. L.; Mannsfeld, S. C.; Ling, M. M.; Liu, S.; Tseng, R. J.; Reese, C.; Roberts, M. E.; Yang, Y.; Wudl, F.; Bao, Z. Patterning Organic Single-Crystal Transistor Arrays. *Nature* **2006**, *444*, 913−917.
(6) Lee, W. H.; Lim, J. A.; Kwak, D.; Cho, J. H.; Lee, H. S.; Choi, H. H.; Cho, K. Semiconductor-Dielectric Blends: A Facile All Solution Route to Flexible All-Organic Transistors. *Adv. Mater.* **2009**, *21*, 4243−4248.
(7) Park, Y. D.; Lim, J. A.; Jang, Y.; Hwang, M.; Lee, H. S.; Lee, D. H.; Lee, H.-J.; Baek, J.-B.; Cho, K. Enhancement of the Field-Effect Mobility of Poly (3-hexylthiophene)/Functionalized Carbon Nanotube Hybrid Transistors. *Org. Electron.* **2008**, *9*, 317−322.
(8) Lee, W. H.; Cho, J. H.; Cho, K. Control of Mesoscale and Nanoscale Ordering of Organic Semiconductors at the Gate Dielectric/Semiconductor Interface for Organic Transistors. *J. Mater. Chem.* **2010**, *20*, 2549−2561.
(9) Soeda, J.; Matsui, H.; Okamoto, T.; Osaka, I.; Takimiya, K.; Takeya, J. Highly Oriented Polymer Semiconductor Films Compressed at the Surface of Ionic Liquids for High-Performance Polymeric Organic Field-Effect Transistors. *Adv. Mater.* **2014**, *26*, 6430−6435.


DOI: 10.1021/acsami.5b00073
*ACS Appl. Mater. Interfaces* 2015, 7, 5898−5906

(10) Tseng, H.-R.; Phan, H.; Luo, C.; Wang, M.; Perez, L. A.; Patel, S. N.; Ying, L.; Kramer, E. J.; Nguyen, T.-Q.; Bazan, G. C.; Heeger, A. J. High-Mobility Field-Effect Transistors Fabricated with Macroscopic Aligned Semiconducting Polymers. *Adv. Mater.* **2014**, *26*, 2993−2998.
(11) Yuan, Y.; Giri, G.; Ayzner, A. L.; Zoombelt, A. P.; Mannsfeld, S. C. B.; Chen, J.; Nordlund, D.; Toney, M. F.; Huang, J.; Bao, Z. Ultra-High Mobility Transparent Organic Thin Film Transistors Grown by an Off-Centre Spin-Coating Method. *Nat. Commun.* **2014**, *5*, 3005.
(12) Wang, C. L.; Dong, H. L.; Hu, W. P.; Liu, Y. Q.; Zhu, D. B. Semiconducting pi-Conjugated Systems in Field-Effect Transistors: A Material Odyssey of Organic Electronics. *Chem. Rev.* **2012**, *112*, 2208−2267.
(13) Duan, C.; Huang, F.; Cao, Y. Recent Development of Push−Pull Conjugated Polymers for Bulk-Heterojunction Photovoltaics: Rational Design and Fine Tailoring of Molecular Structures. *J. Mater. Chem.* **2012**, *22*, 10416−10434.
(14) Ravikumar, C.; Joe, I. H.; Jayakumar, V. Charge Transfer Interactions and Nonlinear Optical Properties of Push−Pull Chromophore Benzaldehyde Phenylhydrazone: A Vibrational Approach. *Chem. Phys. Lett.* **2008**, *460*, 552−558.
(15) Li, Y.; Sonar, P.; Murphy, L.; Hong, W. High Mobility Diketopyrrolopyrrole (DPP)-Based Organic Semiconductor Materials for Organic Thin Film Transistors and Photovoltaics. *Energy Environ. Sci.* **2013**, *6*, 1684−1710.
(16) Nielsen, C. B.; Turbiez, M.; McCulloch, I. Recent Advances in the Development of Semiconducting DPP-Containing Polymers for Transistor Applications. *Adv. Mater.* **2013**, *25*, 1859−1880.
(17) Bijleveld, J. C.; Zoombelt, A. P.; Mathijssen, S. G.; Wienk, M. M.; Turbiez, M.; de Leeuw, D. M.; Janssen, R. A. Poly (diketopyrrolopyrrole−terthiophene) for Ambipolar Logic and Photovoltaics. *J. Am. Chem. Soc.* **2009**, *131*, 16616−16617.
(18) Zhao, Y.; Guo, Y.; Liu, Y. 25th Anniversary Article: Recent Advances in n-Type and Ambipolar Organic Field-Effect Transistors. *Adv. Mater.* **2013**, *25*, 5372−5391.
(19) Guo, X.; Kim, F. S.; Seger, M. J.; Jenekhe, S. A.; Watson, M. D. Naphthalene Diimide-Based Polymer Semiconductors: Synthesis, Structure−Property Correlations, and n-Channel and Ambipolar Field-Effect Transistors. *Chem. Mater.* **2012**, *24*, 1434−1442.
(20) Kim, R.; Amegadze, P. S. K.; Kang, I.; Yun, H.-J.; Noh, Y.-Y.; Kwon, S.-K.; Kim, Y.-H. High-Mobility Air-Stable Naphthalene Diimide-Based Copolymer Containing Extended $\pi$-Conjugation for n-Channel Organic Field Effect Transistors. *Adv. Funct. Mater.* **2013**, *23*, 5719−5727.
(21) Wang, E.; Mammo, W.; Andersson, M. R. 25th Anniversary Article: Isoindigo-Based Polymers and Small Molecules for Bulk Heterojunction Solar Cells and Field Effect Transistors. *Adv. Mater.* **2014**, *26*, 1801−1826.
(22) Stalder, R.; Mei, J.; Graham, K. R.; Estrada, L. A.; Reynolds, J. R. Isoindigo, a Versatile Electron-Deficient Unit For High-Performance Organic Electronics. *Chem. Mater.* **2013**, *26*, 664−678.
(23) Ashraf, R. S.; Kronemeijer, A. J.; James, D. I.; Sirringhaus, H.; McCulloch, I. A New Thiophene Substituted Isoindigo Based Copolymer for High Performance Ambipolar Transistors. *Chem. Commun.* **2012**, *48*, 3939−3941.
(24) Van Pruissen, G. W. P.; Gholamrezaie, F.; Wienk, M. M.; Janssen, R. A. J. Synthesis and Properties of Small Band Gap Thienoisoindigo Based Conjugated Polymers. *J. Mater. Chem.* **2012**, *22*, 20387−20393.
(25) Kim, G.; Kang, S.-J.; Dutta, G. K.; Han, Y.-K.; Shin, T. J.; Noh, Y.-Y.; Yang, C. A Thienoisoindigo-Naphthalene Polymer with Ultrahigh Mobility of 14.4 $cm^2/V{\cdot}s$ That Substantially Exceeds Benchmark Values for Amorphous Silicon Semiconductors. *J. Am. Chem. Soc.* **2014**, *136*, 9477−9483.
(26) Osaka, I.; Saito, M.; Koganezawa, T.; Takimiya, K. Thiophene−Thiazolothiazole Copolymers: Significant Impact of Side Chain Composition on Backbone Orientation and Solar Cell Performances. *Adv. Mater.* **2014**, *26*, 331−338.
(27) Lei, T.; Dou, J. H.; Pei, J. Influence of Alkyl Chain Branching Positions on the Hole Mobilities of Polymer Thin-Film Transistors. *Adv. Mater.* **2012**, *24*, 6457−6461.
(28) Zhang, F.; Hu, Y.; Schuettfort, T.; Di, C.-a.; Gao, X.; McNeill, C. R.; Thomsen, L.; Mannsfeld, S. C.; Yuan, W.; Sirringhaus, H. Critical Role of Alkyl Chain Branching of Organic Semiconductors in Enabling Solution-Processed N-Channel Organic Thin-Film Transistors with Mobility of up to 3.50 $cm^2\ V^{-1}\ s^{-1}$. *J. Am. Chem. Soc.* **2013**, *135*, 2338−2349.
(29) Meager, I.; Ashraf, R. S.; Rossbauer, S.; Bronstein, H.; Donaghey, J. E.; Marshall, J.; Schroeder, B. C.; Heeney, M.; Anthopoulos, T. D.; McCulloch, I. Alkyl Chain Extension as a Route to Novel Thieno [3,2-b] thiophene Flanked Diketopyrrolopyrrole Polymers for Use in Organic Solar Cells and Field Effect Transistors. *Macromolecules* **2013**, *46*, 5961−5967.
(30) Shim, C.; Kim, M.; Ihn, S.-G.; Choi, Y. S.; Kim, Y.; Cho, K. Controlled Nanomorphology of PCDTBT−Fullerene Blends via Polymer End-Group Functionalization for High Efficiency Organic Solar Cells. *Chem. Commun.* **2012**, *48*, 7206−7208.
(31) Chen, H.; Guo, Y.; Yu, G.; Zhao, Y.; Zhang, J.; Gao, D.; Liu, H.; Liu, Y. Highly $\pi$-Extended Copolymers with Diketopyrrolopyrrole Moieties for High-Performance Field-Effect Transistors. *Adv. Mater.* **2012**, *24*, 4618−4622.
(32) Kang, I.; An, T. K.; Hong, J.-a.; Yun, H.-J.; Kim, R.; Chung, D. S.; Park, C. E.; Kim, Y.-H.; Kwon, S.-K. Effect of Selenophene in a DPP Copolymer Incorporating a Vinyl Group for High-Performance Organic Field-Effect Transistors. *Adv. Mater.* **2013**, *25*, 524−528.
(33) Kang, I.; Yun, H. J.; Chung, D. S.; Kwon, S. K.; Kim, Y. H. Record High Hole Mobility in Polymer Semiconductors via Side-Chain Engineering. *J. Am. Chem. Soc.* **2013**, *135*, 14896−14899.
(34) Braunecker, W. A.; Oosterhout, S. D.; Owczarczyk, Z. R.; Larsen, R. E.; Larson, B. W.; Ginley, D. S.; Boltalina, O. V.; Strauss, S. H.; Kopidakis, N.; Olson, D. C. Ethynylene-Linked Donor−Acceptor Alternating Copolymers. *Macromolecules* **2013**, *46*, 3367−3375.
(35) Yun, H.-J.; Choi, H. H.; Kwon, S.-K.; Kim, Y.-H.; Cho, K. Conformation-Insensitive Ambipolar Charge Transport in a Diketopyrrolopyrrole-Based Co-polymer Containing Acetylene Linkages. *Chem. Mater.* **2014**, *26*, 3928−3937.
(36) Schwartz, B. J. Conjugated Polymers as Molecular Materials: How Chain Conformation and Film Morphology Influence Energy Transfer and Interchain Interactions. *Annu. Rev. Phys. Chem.* **2003**, *54*, 141−172.
(37) An, T. K.; Kang, I.; Yun, H. j.; Cha, H.; Hwang, J.; Park, S.; Kim, J.; Kim, Y. J.; Chung, D. S.; Kwon, S. K. Solvent Additive To Achieve Highly Ordered Nanostructural Semicrystalline DPP Copolymers: Toward a High Charge Carrier Mobility. *Adv. Mater.* **2013**, *25*, 7003−7009.
(38) Houk, K. N.; Lee, P. S.; Nendel, M. Polyacene and Cyclacene Geometries and Electronic Structures: Bond Equalization, Vanishing Band Gaps, and Triplet Ground States Contrast with Polyacetylene. *J. Org. Chem.* **2001**, *66*, 5517−5521.
(39) Zhu, Y.; Champion, R. D.; Jenekhe, S. A. Conjugated Donor−Acceptor Copolymer Semiconductors with Large Intramolecular Charge Transfer: Synthesis, Optical Properties, Electrochemistry, and Field Effect Carrier Mobility of Thienopyrazine-Based Copolymers. *Macromolecules* **2006**, *39*, 8712−8719.
(40) Heeger, A.; Sariciftci, N. S. *Primary Photoexcitations in Conjugated Polymers: Molecular Exciton Versus Semiconductor Band Model*; World Scientific: Singapore, 1997.
(41) Ditchfield, R.; Hehre, W. J.; Pople, J. A. Self-Consistent Molecular-Orbital Methods. IX. An Extended Gaussian-Type Basis for Molecular-Orbital Studies of Organic Molecules. *J. Chem. Phys.* **1971**, *54*, 724−728.
(42) Lee, J.; Han, A. R.; Kim, J.; Kim, Y.; Oh, J. H.; Yang, C. Solution-Processable Ambipolar Diketopyrrolopyrrole-Selenophene Polymer with Unprecedentedly High Hole and Electron Mobilities. *J. Am. Chem. Soc.* **2012**, *134*, 20713−20721.
(43) Podzorov, V. Conjugated Polymers Long and winding polymeric roads. *Nat. Mater.* **2013**, *12*, 947−948.


DOI: 10.1021/acsami.5b00073
*ACS Appl. Mater. Interfaces* 2015, 7, 5898−5906

(44) Noriega, R.; Salleo, A.; Spakowitz, A. J. Chain Conformations Dictate Multiscale Charge Transport Phenomena in Disordered Semiconducting Polymers. *Proc. Natl. Acad. Sci. U.S.A.* **2013**, *110*, 16315−16320.
(45) Noriega, R.; Rivnay, J.; Vandewal, K.; Koch, F. P. V.; Stingelin, N.; Smith, P.; Toney, M. F.; Salleo, A. A General Relationship Between Disorder, Aggregation and Charge Transport in Conjugated Polymers. *Nat. Mater.* **2013**, *12*, 1037−1043.
(46) Yang, H.; Shin, T. J.; Yang, L.; Cho, K.; Ryu, C. Y.; Bao, Z. Effect of Mesoscale Crystalline Structure on the Field-Effect Mobility of Regioregular Poly (3-hexyl thiophene) in Thin-Film Transistors. *Adv. Funct. Mater.* **2005**, *15*, 671−676.
(47) Lee, W. H.; Kwak, D.; Anthony, J. E.; Lee, H. S.; Choi, H. H.; Kim, D. H.; Lee, S. G.; Cho, K. The Influence of the Solvent Evaporation Rate on the Phase Separation and Electrical Performances of Soluble Acene-Polymer Blend Semiconductors. *Adv. Funct. Mater.* **2012**, *22*, 267−281.
(48) Lee, W. H.; Park, J.; Kim, Y.; Kim, K. S.; Hong, B. H.; Cho, K. Control of Graphene Field-Effect Transistors by Interfacial Hydrophobic Self-Assembled Monolayers. *Adv. Mater.* **2011**, *23*, 3460−3464.
(49) Kim, J.; Han, A.-R.; Hong, J.; Kim, G.; Lee, J.; Shin, T. J.; Oh, J. H.; Yang, C. Ambipolar Semiconducting Polymers with $\pi$-Spacer Linked Bis-Benzothiadiazole Blocks as Strong Accepting Units. *Chem. Mater.* **2014**, *26*, 4933−4942.
(50) Kalb, W. L.; Mathis, T.; Haas, S.; Stassen, A. F.; Batlogg, B. Organic Small Molecule Field-Effect Transistors with Cytop Gate Dielectric: Eliminating Gate Bias Stress Effects. *Appl. Phys. Lett.* **2007**, *90*, 092104−092104−3.
(51) Yan, H.; Chen, Z.; Zheng, Y.; Newman, C.; Quinn, J. R.; Dötz, F.; Kastler, M.; Facchetti, A. A High-Mobility Electron-Transporting Polymer for Printed Transistors. *Nature* **2009**, *457*, 679−686.
(52) Sakanoue, T.; Sirringhaus, H. Band-Like Temperature Dependence of Mobility in a Solution-Processed Organic Semiconductor. *Nat. Mater.* **2010**, *9*, 736−740.
(53) Minder, N. A.; Ono, S.; Chen, Z.; Facchetti, A.; Morpurgo, A. F. Band-Like Electron Transport in Organic Transistors and Implication of the Molecular Structure for Performance Optimization. *Adv. Mater.* **2012**, *24*, 503−508.
(54) Le Comber, P. G.; Spear, W. E. Electronic Transport in Amorphous Silicon Films. *Phys. Rev. Lett.* **1970**, *25*, 509−511.
(55) Podzorov, V.; Menard, E.; Borissov, A.; Kiryukhin, V.; Rogers, J.; Gershenson, M. Intrinsic Charge Transport on the Surface Of Organic Semiconductors. *Phys. Rev. Lett.* **2004**, *93*, 086602.
(56) Sakanoue, T.; Sirringhaus, H. Band-Like Temperature Dependence of Mobility in a Solution-Processed Organic Semiconductor. *Nat. Mater.* **2010**, *9*, 736−740.
(57) Lee, B.; Chen, Y.; Fu, D.; Yi, H.; Czelen, K.; Najafov, H.; Podzorov, V. Trap Healing and Ultralow-Noise Hall Effect at the Surface of Organic Semiconductors. *Nat. Mater.* **2013**, *12*, 1125−1129.


DOI: 10.1021/acsami.5b00073
*ACS Appl. Mater. Interfaces* 2015, 7, 5898−5906